Effect of Profiles on AC Contamination Flashover Performance of Large-tonnage Suspension Disc Insulators

Hao Yang[1], Jun Zhou[2], Yawei Li[1], Lei Pang[1], Xiaolei Yang[1], Qiaogen Zhang[1] and **Xinzhe Yu[1]**

[1]State Key Laboratory of Electrical Insulation and Power Equipment,
School of Electrical Engineering, Xi'an Jiaotong University,
Xi'an, 710049, PR China
[2]China Electric Power Research Institute
Beijing, 100192, PR China

ABSTRACT

From field experience and laboratory experiments, it was indicated that the flashover performance of contaminated insulators was significantly influenced by the insulator geometry. In the paper, insulators with three different profiles including seven types of deep under-ribs disc insulator, three types of two-shed disc insulator and three types of three-shed disc insulator were tested in an artificial climate chamber to investigate the influences of insulator profile parameters on the flashover performance of large tonnage disc insulators. The artificial contamination test results indicated that 50% flashover voltage stress ($E_{50\%}$) decreased with the increasing insulator diameter and creepage distance. The influence of salt deposit density (*SDD*) was also investigated, and it was found that $E_{50\%}$ of alternating-shed insulator decreased more rapidly than that of deep under-ribs insulator with the increase of *SDD*. An empirical expression was proposed, by employing the least-square method, to describe the relationships between $E_{50\%}$ and insulator configuration parameters as well as *SDD*. Through analyzing the generalized fitting coefficients (*r*) of the equation and the standard error of estimate (*s*), it can be concluded that the calculated results are in good agreement with the experimental data. Moreover, special attentions were also paid to the influence of the under-ribs and the ratio of shed overhang distance to the shed spacing on flashover performance respectively. This work can enrich the investigation of insulators parameters and may provide useful reference for performance evaluation and selection of insulators in EHV and UHV transmission lines.

Index Terms - EHV and UHV, insulator profiles, pollution flashover performance, large-tonnage disc insulator, fitting equation.

1   INTRODUCTION

WITH the increase of voltage level of power system in recent decades, large-tonnage disc suspension insulators are employed to bear the weight of transmission lines and the long insulator strings, especially in EHV and UHV transmission lines [1-3]. For instance, suspension insulators with the specified mechanical load of 300 kN, 400 kN, even 800 kN have been made to meet the increase of power voltage level [2, 4]. In addition, various profiles of insulators have been designed to adapt to the various environments, such as the three outer-ribs were introduced recently [4].

Contamination flashover of outdoor insulators still remains one of the major problems for the transmission lines, even though many works have been done to study the mechanism of arc propagation and predict the flashover voltage [5-8]. For instance, in the early 2004, power outage due to contamination flashover along 500 kV Lines caused great damages in East Grid of China [6].

Service experience and laboratory experiments have shown that the insulator shape has a great influence on the flashover performance of contaminated insulators [1-2, 10-23]. Matsuoka studied the influence of the diameter on ac contamination flashover voltages of station post insulators, and it was proposed that required creepage distance per unit increased with the average diameter [15]. However, the suspension disc insulator string is different from the post station due to the fact that the air gap distance of the former is usually much larger than that of the latter, and the effect of other insulator parameters on the flashover voltage was not involved in literature [15]. Sundarajan demonstrated that the diameter of the insulators had strong influence on the flashover voltage, irrespective of the profile [16]. Whereas, Wang proposed that the disc insulator with alternate long and short under-ribs and a wider gap between the rib tips had a higher flashover voltage and the configurations of the under-ribs had a significant influence on the flashover performance [4]. Farzaneh and Chisholm illustrated a comprehensive check on the influence of insulator parameters on the contaminated flashover performance and gave an empirical equation as follows [1]:

$$E_{50\%} = 52H^{0.2}D^{-0.4}F^{-0.1}(SDD)^{-0.24} \qquad (1)$$

Where, $E_{50\%}$ is 50% flashover voltage, kV/m; H is insulator structure height, mm; D is insulator diameter, mm; F is insulator form factor [27]; SDD is the salt deposit densities, mg/cm^2. Hence, researchers have not come to an agreement on the influence on the insulator flashover performance.

Compared with normal tonnage insulator, the configuration of large-tonnage insulator is larger. The relationship of flashover voltage versus insulator parameters usually acts in a complicated manner (what is called nonlinear) [1-2]. So, it is difficult to predict the flashover performance of large tonnage insulator based on the existing data of the normal tonnage insulator. Moreover, the arc propagation along the insulator surface may be different when the parameters are enlarged, such as the possibility of the spacing bridged by arc may be varied. So far, the investigation of large-tonnage disc insulator with different profiles and configurations has not been reported. Therefore, it is important to research into the influence of profiles on the flashover voltage of the contaminated disc insulator to provide useful reference for performance evaluation and selection of insulators in EHV and UHV transmission lines.

In order to make clear the relationships between flashover performance of contaminated insulators and D, H and creepage distance (L), insulator profiles as well as SDD, several kinds of large-tonnage insulators with various profiles were tested in the climate chamber and the influences of the above factors on flashover performance are analyzed in this paper.

2 EXPERIMENTAL ARRANGEMENTS AND METHODS

2.1 TEST FACILITES

The tests were carried out in the climate chamber in Pollution and Environment Laboratory of China Electric Power Research Institute (CEPRI), and the schematic circuitof

the chamber is shown in Figure 1. The climate chamber, with a size of 12m×12m×12m, could meet the requirements for contamination flashover tests. The power was generated by a 200 kV/5 A, 1000 kVA transformer with a short circuit impedance less than 5% (B in Figure 1). The applied voltage was measured by a capacitive voltage divider, Y, with a voltage ratio of 1000:1. And the leakage current was obtained by measuring the voltage of the sampling resistance, R_S, in series with the specimens, S.
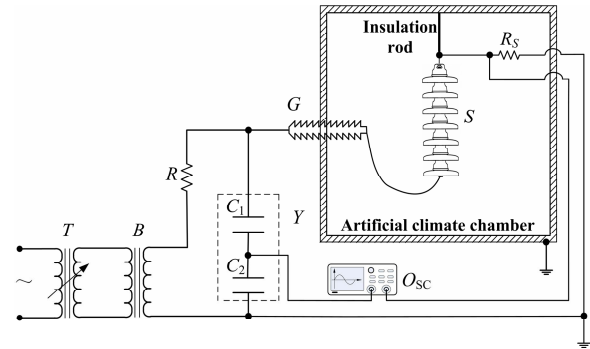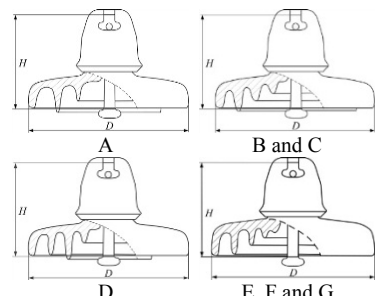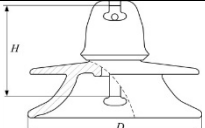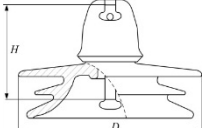

Figure 1. Schematic circuit of CEPRI chamber.

2.2 SPECIMENS

Three profiles of disc insulators as specimens were tested in this paper. Large tonnage insulators of type 1B, 1C, 1D, 1E, 1F, 1G, 2I, 2J, 3K, 3L and 3M, whose configurations and parameters are shown in Table 1, are applied in EHV and UHV transmission lines of China. Type 1A and 2H with a normal specified mechanical load were also tested as a reference to the testing results of large tonnage insulators. Two-shed insulator and three-shed insulator are collectively known as alternating-shed insulator [27].

Table 1. Configurations and parameters of tested insulators

Configurations		Profiles	Type	Shed diameter D/mm	Structure height H/mm	Creepage distance L/mm	Specified mechanical load SML/kN	Form Factor F
A	B and C	Deep under-ribs insulator	1A	288	170	463	210	/
			1B	330	195	490	300	0.900
			1C	386	245	720	530	1.11
			1D	387	235	650	550	0.967
D	E, F and G		1E	320	195	505	300	0.850
			1F	340	205	550	420	1.39
			1G	380	240	695	530	1.01
		Two-shed Insulator	2H	255	146	400	70	/
			2I	330	195	495	300	0.889
			2J	390	205	560	420	0.816
		Three-shed Insulator	3K	400	195	635	300	/
			3L	400	205	635	420	0.846
			3M	400	240	650	550	0.901

2.3 TEST PROCEDURES
2.3.1 PRE-CONTAMINATION

According to the contamination insulator testing standard (IEC60507) [26], the solid-layer method, which has been used to simulate the contamination condition of the insulators in service, was chosen to pollute the insulators. The artificial contamination was a mixture of sodium chloride, kaolin and de-ionized water. The deposit density of kaolin was kept as a constant value of 1mg/cm². The salt deposit densities (*SDD*) were 0.03, 0.05, 0.08 and 0.10 mg/cm² respectively.

2.3.2 ARTIFICIAL FOG

After 24 h natural drying, the specimens were installed in the center of the chamber for 1 h, as shown in Figure 2, to ensure that the temperature of the insulator string was the same as the surrounding before the test. According to IEC60507, steam fog was used for wetting the layer [26]. In the experiments, the steam fog was generated by a 240 kW electric steam boiler with a 0.34 t/h rated steam flow, and was exhausted through the outlet pipes installed on the surrounding walls near the floor. After the applied voltage reached the desired value, the outlet pipes were turned on and the flow of steam fog was kept at a constant value of 0.157 kg/h·m³. According to the change of the largest leakage current value of each minute during one single withstand test, the humidity of the insulator surface reached saturated after about 20 min~30 min after the application of the steam fog. It was found that the temperature rise in the test chamber did not exceed 15 K by the end of the test, which met the requirements mentioned in IEC60507.

Figure 2. Specimens installation

2.3.3 IMAGES RECORDING

In order to study the process of the arc propagation along the insulator surface, an ultra-high speed camera with a speed of 1000 fps was employed. To avoid fuzzy vision caused by the steam fog in the recording of the arc process, the images were recorded in the cold fog condition.

2.3.4 THE 50% FLASHOVER VOLTAGE $U_{50\%}$

The 50% contamination flashover voltage $U_{50\%}$ was determined by adopting the up-and-down method [26-27], and the voltage step adopted in the experiments was 5% of the estimated $U_{50\%}$. For one experiment, the voltage was kept on for 60 min or until the occurrence of flashover. More than ten valid tests were carried out, and the $U_{50\%}$ could be calculated as follows:

$$U_{50\%} = \frac{\sum_{i=1}^{C} c_i U_i}{C} \tag{2}$$

Where, U_i is the voltage value; c_i is the number of tests carried out at voltage level U_i; C is the total number of the valid tests. The 50% flashover voltage per unit ($U_{50\%}/N$) can be obtained by dividing $U_{50\%}$ by N, which is the number of insulators of the tested insulator string. And 50% flashover voltage stress, $E_{50\%}$, which can reflect the utilization ratio of L [5], is obtained by dividing the flashover voltage by the creepage distance of the tested insulator string.

$$E_{50\%} = \frac{U_{50\%}}{l} \tag{3}$$

Where, l is the creepage distance of the insulator string and L multiplied by N equals to l.

3   TEST RESULTS AND ANALYSIS

3.1 INFLUENCE OF INSULATOR CONFIGURATION PARAMETERS

The $E_{50\%}$ values of six types of deep under-ribs insulators are shown in Figure 3. It can be concluded that $E_{50\%}$ tends to decrease approximately when D increases from 288 mm to 386 mm.
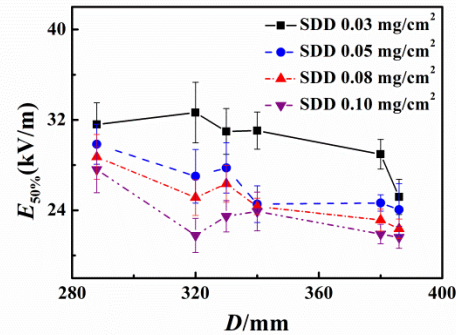
Figure 3. $E_{50\%}$ of deep under-ribs disc insulator versus D at various *SDD*s

A typical surface expansion graph of deep under-ribs insulator is shown in Figure 4. The increase in D results in the increase of channel diameter of pollution layer, which leads to the decrease of surface resistance. According to Obenaus model, any decrease in the resistance of the pollution layer will reduce the flashover voltage [1]. Hence, $E_{50\%}$ decreases with the increase of D. However, an increase in diameter does not reduce flashover voltage correspondingly when *SDD* is higher. It was proposed by Sundararajan that this is due to the increase in the number of arcs initiated with increasing diameter, causing a higher electrode voltage drop that partially compensates for the increase in flashover voltage [16].

Figure 4. The surface expansion graph of deep under-ribs disc insulator.

The $U_{50\%}$ values of the tested insulator versus L are shown in Figure 5. Because larger dimensions are employed in the designing of large-tonnage insulators, the flashover voltage of

large-tonnage insulator is higher than that of normal-tonnage insulator (type 1A and type 2H), which meets the requirements in EHV and UHV transmission lines. The results show that $U_{50\%}/N$ increases with L, but the increase tendency becomes saturated when L is larger than 650 mm. It can be assumed that L=650 mm is the appropriate value for the designing of large-tonnage under-rib disc insulator.
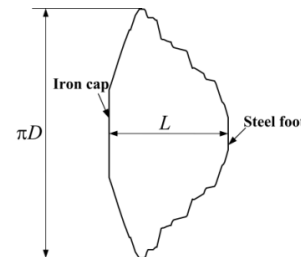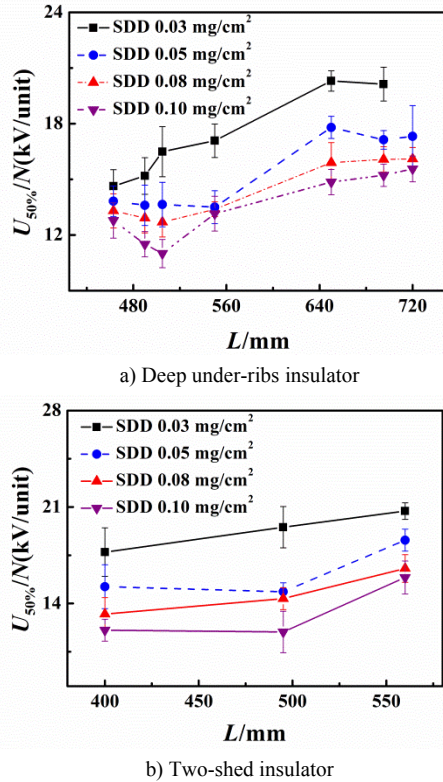

a) Deep under-ribs insulator

b) Two-shed insulator

Figure 5. $U_{50\%}/N$ versus L at various *SDD*s.

On the contrary, the $E_{50\%}$ value decreases with the increase of L. It can be seen from Figure 6 that $E_{50\%}$ decreases roughly with the increase of L, which means that the utilization ratio of L decreases when L becomes larger.   And the descending rate of the curve increase when L is larger than 650 mm, which is corresponding to the saturated point in Figure 5. This is due to the fact that the possibility of air gap being bridged by arc grows up with increasing L, causing a lower utilization ratio of L. It is suggested that the flashover voltage and the utilization of L should be both taken into account in the designing of EHV and UHV insulator strings.

For large-tonnage insulator, the values of H are usually set to a large value in the designing to prevent the spacing from being broken down easily. In fact, in the designing of large-tonnage insulator, the H values don't vary distinctly. The $E_{50\%}$ values of three-shed insulator are compared in Figure 7, and it can be observed that $E_{50\%}$ of three-shed insulators varies with H slightly when H ranges from 195 mm to 240 mm. It can be concluded from equation (1) that $E_{50\%}$ increase with H, and the increase rate tends to be saturated when H is large. The arc bridging between the spacing can be totally avoided when H is large enough, and the fact that the arc only propagates along the insulator surface leads to the constancy of $U_{50\%}$ values as well as the sharp decrease of $E_{50\%}$ with the continuously increasing H. It can be indicated that the

relationship between $E_{50\%}$ and H tends to be a dromedary curve. It may be assumed that the H values of large-tonnage insulators locate in the range of the curve peak, causing the little variation shown in Figure 7.
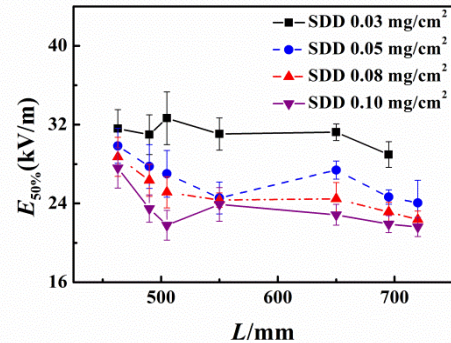
Figure 6. $E_{50\%}$ versus L of deep under-ribs insulators at various *SDD*s
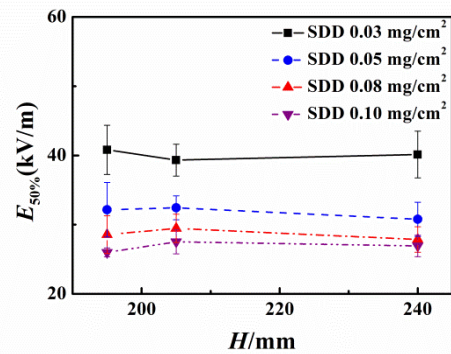
Figure 7. $E_{50\%}$ versus H of three-shed insulators at various *SDD*s.

3.2 INFLUENCE OF INSULATOR PROFILES

Type 1B, 1D, 1E and 1G are deep under-ribs insulators. Besides, type 2I is two-shed insulator and type 3M is three-shed insulator. The three configuration parameters, D, H and L, of type 1B, 1E and 2I are quite similar, so are for type 1D, 1G and 3M. The comparison of flashover voltage of deep under-ribs disc insulators and alternating-shed insulators with similar configuration parameters is shown in Figure 8. It can be concluded that the $U_{50\%}/N$ values of alternating-shed disc insulators are higher than that of deep under-ribs disc insulators, especially when *SDD* is lower.

It is found that spacing amid the ribs of the deep under-ribs insulator is easily bridged by arc. The images of air gap amid the under-ribs bridged by arc (shot from a lower slanting position) and the schematic diagrams are shown in Figure 9. However, for alternating-shed insulator, the arc propagates along the outer shed and the spacing between the outer sheds is much larger. Therefore, the possibility of air gap being bridged by arc is smaller, and the utilization ratio of L of alternating-shed disc insulator is higher than that of deep under-ribs disc insulator, resulting in the lower $U_{50\%}/N$.

Furthermore, the $E_{50\%}$ values of insulators with various profiles and different configuration parameters are investigated and the results are shown in Figure 10. It can also be noted that $E_{50\%}$ of alternating-shed insulator is higher than that of deep under-ribs insulator. And it can be observed that the $E_{50\%}$ of three-shed insulator shows a little advantage over that of two-shed insulator. This may be due to the existence of

the middle shed of the three-shed insulator hindering the arc bridging in the shed spacing, causing the improvement of utilization ratio of L.

(a) $U_{50\%}/N$ of type 1B, 1E and 2I

(b) $U_{50\%}/N$ of type 1D, 1G and 3M

Figure 8. Comparison of $U_{50\%}/N$ of deep under-ribs disc insulator and alternating-shed insulator.

Figure 9. The images of spacing amid the under-ribs bridged by arc and the schematic diagram.

Figure 10. Comparison of $E_{50\%}$ of deep under-ribs disc insulator and alternating-shed insulator.

3.3 INFLUENCE OF *SDD*

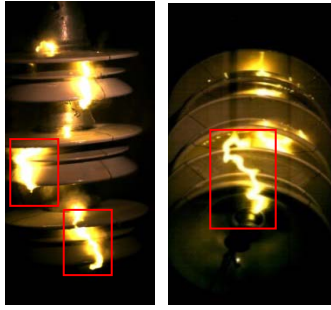Many works have been done to investigate the influence of *SDD* on insulator flashover voltage. Previous researches showed that the relationships between *SDD* and 50% flashover voltage stress can be described as follows [1, 5]:

$$E_{50\%} \propto (SDD)^{-n} \tag{4}$$

Where, n is the exponential factor related to influences of *SDD* on the flashover voltage. The generalized correlation coefficient r reflecting how well the nonlinear estimated equation fits the sample data is defined as follows [28]:

$$r = \sqrt{1 - \sum_{i=1}^{m}\left(E_{50\%i} - \hat{E}_{50\%i}\right)^2 / \sum_{i=1}^{m}\left(E_{50\%i} - \overline{E}_{50\%}\right)^2} \tag{5}$$

Where, $E_{50\%i}$ is the test result; $\hat{E}_{50\%i}$ is the estimated value of the fitting equation; $\overline{E}_{50\%i}$ is the average value of the test results; m is the number of the data. The standard error of estimate s is defined as follows [28]:

$$s = \sqrt{\frac{\sum_{i=1}^{m}\left(E_{50\%i} - \hat{E}_{50\%i}\right)^2}{m}} \tag{6}$$

The exponential factor n and generalized fitting coefficients r of the tested insulators are shown in Table 2. The n values of alternating-shed insulators are higher than that of deep under-ribs insulator, which means that the influence of *SDD* on flashover performance of alternating-shed insulator is significant and $E_{50\%}$ decreases more rapidly with increasing *SDD*. The comparison can be observed from Figure 8 and 10 in last section. This may be due to the fact that the arc levitation is severe making part of L of alternating-shed insulator ineffective when *SDD* is higher. It is reported that ionization mode of arc plasma is mainly thermal ionization [24]. In case of higher *SDD*, the leakage current is larger, and the injection energy for partial arc is higher compensating for the increase of ionization degree as well as arc temperature and decrease of particle density of arc plasma [25]. The arc, driven by electric field force and thermal buoyancy, may deviate from the polluted insulator surface easily leading to the shed spacing of alternating-shed insulator bridged by arc and the decrease of $E_{50\%}$, as shown in Figure 11. As to deep under-ribs insulator, the path of arc propagation is similar to Figure 9, so that the "shorting out" creepage distance by arc of deep under-ribs insulator is shorter than that of alternating-shed insulator. Hence, the influence of *SDD* on alternating-shed insulator is significant and $E_{50\%}$ decreases more rapidly with increasing *SDD*.

Table 2. Parameters of tested disc insulators.

Insulator	Deep under-ribs			Two-shed		Three-shed	
	1B	1D	1G	2I	2J	3K	3M
n	0.193	0.256	0.24	0.426	0.304	0.371	0.346
r	0.969	0.999	0.991	0.938	0.984	0.987	0.955

Figure 11. Arc levitation of three-shed insulator.

3.4 EMPIRICAL FITTING EQUATION OF $E_{50\%}$

The empirical equation (1) proposed in literature [1] has taken the insulator profile parameters into account to predict $E_{50\%}$, and it is employed to calculate the $E_{50\%}$ results of the specimens tested in this paper. The comparisons between the test results and the estimated values of three representative types of insulators (type 1G, type 2I and type 3L) are shown in Figure 12. It can be concluded that the calculated results (CR) match relatively well with the experimental data of two-shed insulator by analyzing the standard error s of the estimate value. However, the CR of equation (1) for deep under-ribs large-tonnage insulator is higher than experimental data and CR for three-shed large-tonnage insulator is lower than the experimental data. According to equation (1), $E_{50\%}$ decreases with the increase of F. But for large-tonnage insulator, the relationship between F and $E_{50\%}$ under SDD=0.03 mg/cm^2 is shown in Figure 13, and it can be concluded that there is no obvious regular relation between F and $E_{50\%}$ when F lies between 0.816 and 1.39.
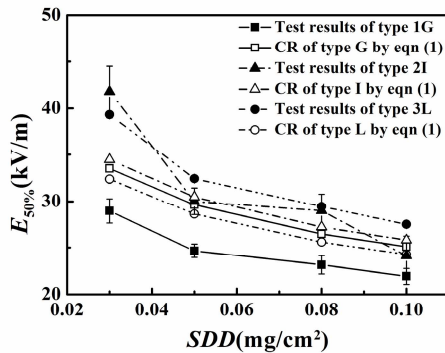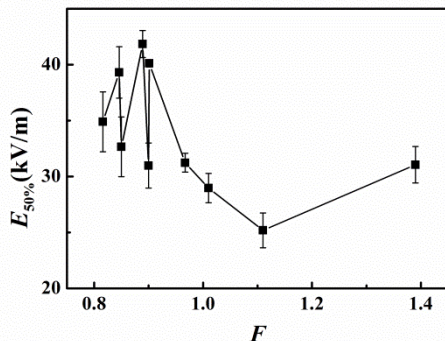

Fig. 12 The comparisons between the tested data and empirical fit proposed by literature [1].

Fig. 13 The $E_{50\%}$ values versus F of large-tonnage insulator under SDD=0.03 mg/cm^2.

As mentioned above, the flashover performance of insulator is related to D, L, SDD and insulator profiles intensively. On the contrary, $E_{50\%}$ varies with H slightly and doesn't have an obvious and regular relationship with F. Previous researches have shown that the flashover performance varied in an exponential relationship with insulator configuration parameters [1-2, 15]. Hence, the expression of $E_{50\%}$, which is intended to have the physical meanings corresponding to the test results, is described as follows:

$$E_{50\%} = kD^{-\alpha}L^{-\beta}(SDD)^{-\gamma} \qquad (7)$$

Where, the coefficient k represents the profile of the insulator on $E_{50\%}$. And for under-rib insulator, two-shed insulator and three-shed insulator k equals k_1, k_2 and k_3 respectively; α, β and γ are three indexes, which represent D, L and SDD on the $E_{50\%}$ respectively, to be determined. As mentioned in Section 3.3, the influences of SDD on flashover performance of these three profiles of insulator are different. Therefore, for under-rib insulator, two-shed insulator and three-shed insulator, γ equals γ_1, γ_2 and γ_3. After taking logarithm, the following equation is obtained:

$$\begin{cases} \lg E_{50\%} = \lg k_1 - \alpha \lg D - \beta \lg L - \gamma_1 \lg SDD & (8-1) \\ \lg E_{50\%} = \lg k_2 - \alpha \lg D - \beta \lg L - \gamma_2 \lg SDD & (8-2) \\ \lg E_{50\%} = \lg k_3 - \alpha \lg D - \beta \lg L - \gamma_3 \lg SDD & (8-3) \end{cases} \quad (8)$$

Based on the least-square method, as long as the sum of squares of deviation Q is as minimum as possible, the absolute error between the test data and the calculated values will be small enough. Q corresponding to equation (8-1) is expressed as follows:

$$Q = \sum_{i=1}^{n}\left[\lg(E_{50\%})_i - \left(\lg k_1 - \alpha \lg D_i - \beta \lg L_i - \gamma_1 \lg SDD_i\right)\right]^2 \quad (9)$$

According to the disciplines of least square method, the following the constraint condition is obtained:

$$\frac{\partial Q}{\partial \alpha} = \frac{\partial Q}{\partial \beta} = \frac{\partial Q}{\partial \gamma_1} = \frac{\partial Q}{\partial (\lg k_1)} = 0 \qquad (10)$$

Based on the tested results, the coefficients in the equation (8-1) are determined combining the equations (9) and (10). By employing the similar method, all the residual coefficients are obtained, and $E_{50\%}$ of large-tonnage disc insulator is described as follows:

$$E_{50\%} = \begin{cases} 805 \cdot D^{-0.63} \cdot L^{-0.05} \cdot SDD^{-0.20} & \text{Deep under-rib insulator} \\ 592 \cdot D^{-0.63} \cdot L^{-0.05} \cdot SDD^{-0.36} & \text{Two-shed disc insulator} \\ 724 \cdot D^{-0.63} \cdot L^{-0.05} \cdot SDD^{-0.34} & \text{Three-shed disc insulator} \end{cases} \quad (11)$$

It is suggested by the obtained empirical fit equation (11) that D plays a more important role in $E_{50\%}$ than either L or SDD, which is corresponding to the conclusion mentioned in literature [1].

The generalized fitting coefficients r values together with s values of all the tested insulators are shown in Table 3. It can be concluded that CR of equation (11) are in relatively good agreement with the experimental data. In order to compare with the results shown in Figure 12, tested results and CR of equation (11) of type 1G, 2I with 3L are compared in Figure 14, which can ensure the correctness of the given equation. However, the estimate value of type 1C deviates from the test data, and this will be discussed in the following section.
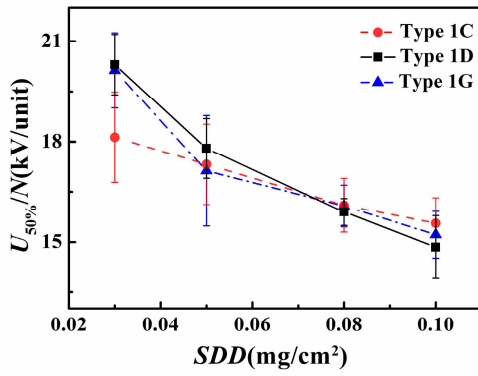
Table 3. The *r* and *s* values of the tested insulators.

Insulator type	1A	1B	1C	1D	1E	1F	1G	2H	2I	2J	3K	3L	3M
r	0.802	0.958	0.742	0.821	0.908	0.967	0.943	0.967	0.939	0.803	0.980	0.978	0.968
$s/\text{kV} \cdot \text{m}^{-1}$	1.27	0.78	3.55	2.83	1.65	1.38	2.16	1.38	2.24	0.94	1.13	0.94	1.32

Fig. 14 The comparisons between the tested data and the CR of equation (10) in this paper.

Moreover, the tested results and the CR of three types of insulator under *SDD*=0.2 mg/cm^2 are compared, which are shown in Figure 15. Also, a new three-shed insulator is used as a reference to check the accuracy of the given empirical fit equation, and the comparisons are shown in Figure 16. It can be concluded from the comparison between test results and the predicted values that the CR of equation (11) are in good agreement, and the adoption of equation (11) as the prediction of insulator flashover performance is reasonable.

Fig. 15 The comparisons between the tested data and CR under 0.02 mg/cm^2.

Fig. 16 The comparisons between the tested data and CR of a new three-shed insulator under 0.02 mg/cm^2.

4   DISCUSSIONS

The empirical equation obtained in the Section 3.4 is intended to give a globe check on the performance of the contaminated insulators and provide a comprehensive reference for performance evaluation and selection of insulators in EHV and UHV transmission lines. Nevertheless, some exceptions and interesting phenomena have been noticed and will be discussed in this part.

4.1   DEEP UNDER-RIBS DISC INSULATORS WITH AN EXTRA RIB

It has been reported that DC insulator with a group of alternate long and short under-ribs has a higher flashover voltage, for the adoption of alternate under-ribs can increase the *L* value and the length of insulator spacing of the under-ribs [4]. And it is also reported that the extra under-rib can hinder the arc propagation, even inhibit the arc levitation [2, 4].

The parameters *D*, *H* and *L* of type 1C, 1D and 1G, which are deep under-ribs disc insulator, are quite similar, but type 1C and 1D have an extra under-rib, as shown in Figure 17. The $U_{50\%}/N$ results versus *SDD* of these three types of disc insulator are shown in the Figure 18. It can be observed that the performance of deep under-ribs disc insulator with an extra under-rib doesn't show an obvious advantage over the insulator without an extra under-rib. On the contrary, the $U_{50\%}/N$ of type 1C is obviously lower than that of two other types when *SDD* is 0.03mg/cm^2.

Although the gap distance of under-ribs and *L* of the insulator increase by introducing extra under-rib, the existence of the extra under-rib shorten the spacing distance of successive insulator sheds, thus the air gap is easy to be broke down by arc. It is shown in Figure 19 that the air gap of type 1C between the secondary external extra under-rib and the insulator shed below is broken down by the arc when *SDD* is 0.03 mg/cm^2, and the big dispersion of the flashover voltage indicates that there is a possibility in the breakdown of the spacing.

Figure 17. Type 1C, 1D and 1G insulator.

Figure 18. Comparison of $U_{50\%}/N$ of deep under-ribs disc insulator with and without extra rib.
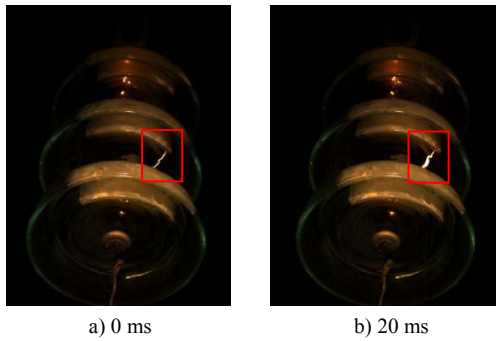

|a) 0 ms|b) 20 ms|

Figure 19. Images of air gap being bridged by arc of type 1C insulator.

Nevertheless, the arc bridging shown in Figure 19 can't be captured when *SDD* is higher, which is corresponding to the results in Figure 18. As shown in Figure 20, there are two possible leakage paths for arc to propagate from the tip of extra rib (Point a) to the insulator shed below (Point d): Path 1 is the breakdown of air gap, and the breakdown voltage is defined as U_{ad}; Path 2 includes a→b and c→d (the electrical potential values of Point b and Point c are equal), the surface flashover voltages of a→b and c→d, which decrease with the increasing *SDD*, are defined as U_{ab} and U_{cd} respectively. If *SDD* is lower, then

$$U_{ab} + U_{cd} > U_{ad} \tag{12}$$

The arc will propagate along Path 1, and the air gap is broken down corresponding to Figure 19. When *SDD* is higher, the values of U_{ab} and U_{cd} become lower. Until,

$$U_{ab} + U_{cd} < U_{ad} \tag{13}$$

The arc will pass along Path 2, and the phenomena of arc bridging are avoided. Hence, the arc bridging has not been caught under higher *SDD* values.

Figure 20. Two possible paths.

Both type 1C and type 1D insulators have an extra under-rib, however, the phenomena of the shed spacing between the extra under-rib and the insulator shed below of type 1D being bridged by the arc have not been captured in the ten times of recording. And this is corresponding to the result that flashover voltage of type 1D is higher than that of type 1C. Extra rib of type 1D is in an inner position causing the distance of a→b and c→d becomes shorter and equation (13) holds for all the *SDD*s selected in this test. Hence, the breakdown of Path 1 has not been captured. In addition, the electric field around the extra under-rib tips of type 1C and type 1D is analyzed by employing Ansoft®. The highest electric field strength around the extra rib of type 1C insulator is 40% higher than that of type 1D, as shown in Figure 21. Hence, the inception of discharge around the tip of type 1C is much easier leading to the breakdown of the air gap easily.

|a) Type 1C|b) Type 1D|
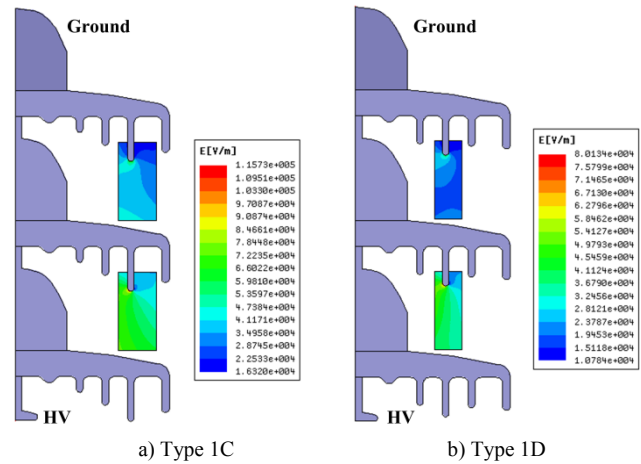
Figure 21. Electric field around extra rib of type 1C and 1D.

Accordingly, the configuration of type 1C should be optimized to improve the flashover performance when *SDD* is lower. It is suggested that the distance of the spacing between the tip of the extra under-rib and the successive insulator shed below should be considered to prevent the air gap from being broken down easily when designing the under-rib disc insulator with alternate under-ribs.

4.2 FLASHOVER PERFORMANCE OF TWO-SHED INSULATOR

The $E_{50\%}$ values of two-shed insulator are discussed in this part. It can be remarked from Figure 22 that $E_{50\%}$ of type 2I is lower than that of type 2H and type 2J.
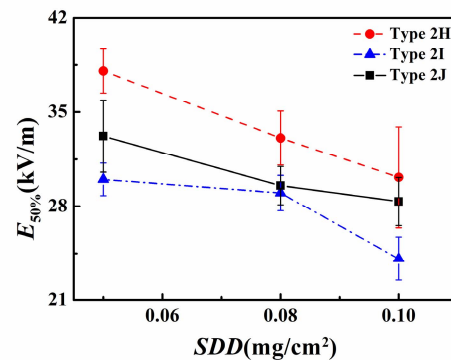

Figure 22. $E_{50\%}$ of two-shed insulators.

The arc propagation images of the two-shed insulator strings are investigated to explain the reason. It can be observed from the highlighted parts in Figure 23 that the air gap amid the two sheds and the air gaps amid the two insulators are bridged by the arc. The schematic diagrams of two ways of arc bridging the air gaps are shown in Figure 24. If the ratio of shed overhang distance to the shed spacing is not appropriate, the possibility of the spacing bridged by shed-to-shed arc is higher causing the decrease in the utilization ratio of *L*. The ratio of shed overhang distance to the shed spacing of type I insulator maybe lies in the range where the possibility of the spacing being bridged by arc is high. And this is corresponding to researches conducted by Li on a glass model [8]. Because the shed-to-shed spacing are important for the avoidance of "shorting out" creepage distance bridged by a shed-to-shed arc [27], the influence of the ratio of shed overhang distance to the shed spacing on the two-shed insulator flashover performance will be studied in the future.

a) 0 ms   b) 20 ms   c) 40 ms   d) 60 ms

a) 0 ms   b) 20 ms   c) 40 ms
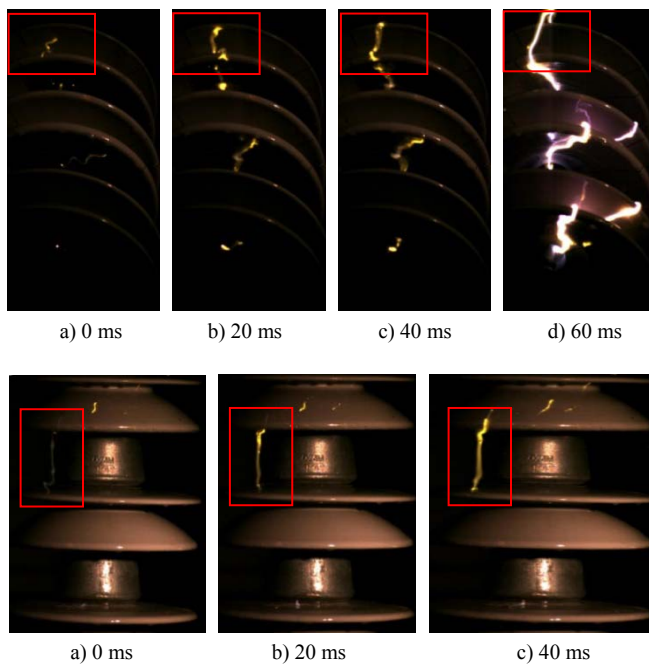
Figure 23. Arc propagation along the insulator surface.
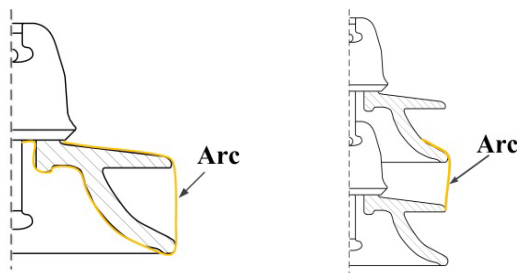
Figure 24. The schematic diagram of two ways of the spacing being broken down by arc.

5   CONCLUSIONS

The effect of profiles on contamination flashover performance of AC large-tonnage disc suspension insulators is

investigated in this paper, and the following conclusions are obtained.

(1) The $E_{50\%}$ values of large-tonnage insulator decrease with the increase of diameter and creepage distance. It is also found that $E_{50\%}$ of alternating-shed insulator decreases more rapidly than that of deep under-ribs insulator with the increase of *SDD*. The flashover voltage of alternating-shed disc insulator is higher than deep under-ribs disc insulators when the insulator configuration parameters are similar.

(2) Considering the obtained experimental relations, an empirical fit equation describing the relationships between $E_{50\%}$ was given in this paper, and the comparison results showed that the calculated results were in good agreement with the test results. From the comparisons of the predicted results and the test results, it was shown that the evaluation of the flashover performance by employing the proposed empirical equation was reasonable.

(3) The under-rib disc insulator with an extra under-rib doesn't show an obvious advantage in flashover performance. Oppositely, the existence of the extra under-rib shortens the air gap, causing the air gap being easily broke down by arc compensating for a lower flashover voltage. For two-shed disc insulator, it is suggested that the ratio of shed overhang distance to the shed spacing should be optimized, otherwise the shed-to-shed spacing will be bridged by arc, leading to the "shorting out" creepage distance and a lower utilization ratio of *L*.

4) All the conclusions in this paper are were drawn under atmospheric pressure. For the EHV and UHV transmission lines in China may pass through some high altitude area, the influence of pressure will be considered in the investigations of profiles on the insulator performance in our further studies.

ACKNOWLEDGMENT

REFERENCES

[1] M. Farzaneh and W. Chisholm, *Insulators for Icing and Polluted Environments*, 1st ed., IEEE Press: New Jersey, pp. 211-239, 2009.

[2] Z. Guan, *Insulators and Outdoor Insulation*, 1st ed., Tsinghua Press: Beijing, pp. 15-17, 2006 (in Chinese).

[3] Y. Liu, Z. Su and B. Wang, "The design performance of DC Suspension Insulators", Insulators and Surge Arresters, Vol. 6, pp. 1-8, 1988 (in Chinese).

[4] B. Wang, "Design Performance and Application of DC Suspension Porcelain Insulators", Insulators and Surge Arresters, Vol. 1, pp. 13-18, 2010 (in Chinese).

[5] C. Zhang, L. Wang, Z. Guan and F. Zhang, "Pollution Flashover Performance of Full-scale ±800kV Converter Station Post Insulators at High Altitude Area", IEEE Trans. Dielectr. Electr. Insul., Vol. 20, pp. 200-208, 2012.

[6] Z. Guan, S. Wang, X. Liang, L. Wang and J. Fan, "Application and Prospect of Polymeric Outdoor Insulation in China", High Voltage Technology, Vol. 26, pp. 37-39, 2000 (in Chinese).

[7] C. Zaniani, *Dynamic Modeling of ac Arc Development on ice surfaces*, Ph.D. thesis, UQAC, 2004.

[8] J. Li, *Study of the Mechanism of Arc Propagation over a Polluted Insulation Surface and Time-varying Model*, Ph.D. thesis, Tsinghua University, 2013 (in Chinese).

[9] F. Topalis, I. Gonos and I. Stathopulos, "Dielectric Behaviour of Polluted Porcelain Insulators", IEE Proc.-Gener. Transm. Distrib., Vol. 148, pp. 269-274, 2001.

[10] C. Engelbrecht, I. Gutman, and R. Hartings, "A Practical Implementation of Statistical Principles to Dimension AC Line Insulators With Respect to Contaminated Conditions", IEEE Trans. Power Del., Vol. 22, pp. 667-673, 2007.

[11] V. Kontargyri, A. Gialketsi, G. Tsekouras, I. Gonos, I. Stathopulos, "Design of an Artificial Neural Network for the Estimation of the Flashover Voltage on Insulators", Elsevier Electr. Power Syst. Res., Vol. 77, pp. 1552-1560, 2007.

[12] Y. Li, *Influences of AC Partial Arc on Contaminated Flashover Characteristics of Insulator Strings*, Ph. D. thesis, Xi'an Jiaotong University, 2013 (in Chinese).

[13] F. Zhang, L. Wang, Z. Guan and M. MacAlpine, "Influence of Composite Insulator Shed Design on Contamination Flashover Performance at High Altitudes", IEEE Trans. Dielectr. Electr. Insul., Vol. 18, No. 3; June 2011.

[14] T. Cheng and H. Nour, "A Study on the Profile of HVDC Insulators: Mathematical Modeling and Design", IEEE Trans. Electr. Insul., Vol. 24, pp.113-117, 1989.

[15] R. Matsuoka, S. Ito, K. Sakanishi and K. Naito, "Flashover on Contaminated Insulators with Different Diameters", IEEE Trans. Electr. Insul., Vol. 26, pp. 1140-1146, 1991.

[16] R. Sundarajan and R. Gorur, "Effect of Insulator Profiles on dc Flashover Voltage under Polluted Conditions: A Study using a Dynamic Arc Model*"*, IEEE Trans. Dielectr. Electr. Insul., Vol. 1, pp. 124-132, 1994.

[17] H. Mei, J. Chen, G. Peng, J. Li, L. Wang and Z. Guan, "Pollution Flashover Characteristic of Composite Insulators Installed Extra Large Sheds", High Voltage Engineering, Vol. 37, pp. 606-612, 2011 (in Chinese).

[18] K. Naito, K. Morita, Y. Hasegawa, and T. Imakoma, "Improvement of the dc Voltage Insulation Efficiency of Suspension Insulators under Contaminated Conditions", IEEE Trans. Dielectr. Electr. Insul., Vol. 23, pp. 1025-1032, 1988.

[19] X. Jiang, J. Yuan, J. Zhang, J. Hu and C. Sun "Study on AC Artificial-Contaminated Flashover Performance of Various Types of Insulators", IEEE Trans. Power Del., Vol. 22, pp. 2567-2573, 2007.

[20] Q. H, L. Shu, X. Jiang, C. Sun, J. Zhang and J. Hu, "Effects of Shed Configuration on AC Flashover Performance of Ice-covered Composite Long-rod Insulators", IEEE Trans. Dielectr. Electr. Insul., Vol. 19, pp. 124-132, 1994.

[21] X. Jiang, L. Shu, Y. Zhang, J. Zhang and J. Hu, "Influence of ESDD and NSDD on AC Flashover Characteristic of Artificially Polluted XP-160 Insulators", Proceedings of the CSEE, Vol.26, pp. 24-28, 2006 (in Chinese).

[22] L. Shu, Q. Ran, X. Jiang, J. Zhang and J. Hu, "Comparison of AC Artificial Pollution Flashover Performance Between Porcelain and Glass Insulators", High Voltage Engineering, Vol.33, pp. 9-13, 2007 (in Chinese).

[23] K. Siderakis, D. Agoris, J. Stefanakis and E. Thalassinakis, "Influence of the Profile on the Performance of Porcelain Insulators Installed in Coastal High Voltage Networks in the Case of Condensation Wetting", IEE Proc.-Sci. Meas. Technol., Vol. 153, pp. 158-163, 2006.

[24] F. Guo, *Study on the Streamer Characteristics along the Polluted Insulation Surface and the Development Arc Energy Balance Model under DC Voltage*, Ph.D. thesis, Chongqing University, 2012 (in Chinese).

[25] A. Nekahi, *Spectroscopic Investigation of Arc over an Ice Surface*, Ph.D. thesis, UQAC, 2011.

[26] Artificial Pollution Tests on High-voltage Insulators to be Used on A.C. Systems, IEC 60507: 1991.

[27] Selection and Dimensioning of High-voltage Insulators Intended for Use in Polluted Conditions, IEC/T 60815:2008.

[28] M. Spiegel, J. Schiller and R. Srinivasan, *Probability and Statistics*, 3rd ed., The McGraw-Hill Companies Incorporated: New York, pp. 265-314, 2009.
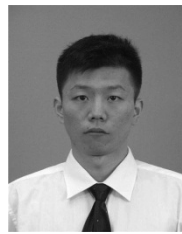
Hao Yang was born in Hebei Province, China in 1988. He received the B.Sc. degree from the School of Electrical Engineering, Xi'an Jiaotong University, China, in 2011. He is currently working toward a Ph.D degree at the High Voltage Division, School of Electrical Engineering, Xi'an Jiaotong University. His major research interests include outdoor insulation.

Jun Zhou was born in Jiangsu Province, China, in 1973. He received the Ph.D. degree from Tsinghua University, China, in 2004. After graduation, he worked in China Electric Power Research Institute. His major research field is external insulation, especially in UHV areas.
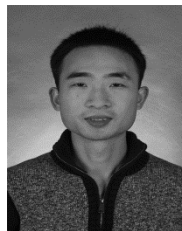
Yawei Li was born in Henan Province, China in 1980. He received the B.Sc. and M.Sc. degrees from the School of Material Engineering, Henan University of Science and Technology and School of Electrical Engineering, Sichuan University, China, in 2004 and 2007 respectively. He is currently working toward a Ph. D degree at High Voltage Division, School of Electrical Engineering, Xi'an Jiaotong University. His major research interests include outdoor insulation.

Lei Pang was born in Shanxi province,China, in 1981. He received the B.Sc., M.Sc. and Ph.D. degrees from Xi'an Jiaotong University, Xi'an, China, in 2004, 2007, and 2013, respectively. He is currently pursuing a post-doctorate in high voltage technology in Xi'an Jiaotong University. His major research interests include outdoor insulation.

Xiaolei Yang was born in Sichuan Province, China, in 1988. He received the B.Sc. degree in electrical engineering from Xi'an Jiaotong University, Xi'an, China, in 2012. He is currently working toward a M.Sc. degree at the High Voltage Division, School of Electrical Engineering, Xi'an Jiaotong University.

Qiaogen Zhang was born in Jiangsu Province, China, in 1965. He received the B.Sc., M.Sc., and Ph.D. degrees from Xi'an Jiaotong University, Xi'an, China, in 1988, 1991, and 1996, respectively. He is currently a professor with the State Key Laboratory of Electrical Insulation and Power Equipment, School of Electrical Engineering, Xi'an Jiaotong University. His major research interests include outdoor insulation, pulse power technology, gas discharge and its application.

Xinzhe Yu was born in Tianjin, China, in 1983. He received the B.Sc. and M.Sc. degrees in electrical engineering from Xi'an Jiaotong University, Xi'an, China, in 2008 and 2011, respectively. After graduation, he worked in China Electric Power Research Institute. He is currently working toward an on-the-job Ph.D. degree at the High Voltage Division, School of Electrical Engineering, Xi'an Jiaotong University. His major research interests include outdoor insulation.